

Kinetic Effects in the Collisionless Expansion of Spherical Nanoplasmas

F. Peano¹, F. Peinetti¹, R. Mulas¹, G. Coppa¹ and L.O. Silva²

¹ *Dipartimento di Energetica, Politecnico di Torino, Italy*

² *GoLP/Centro de Física dos Plasmas, Instituto Superior Técnico, Lisboa, Portugal*

Abstract. The collisionless expansion of spherical plasmas (cold ions plus hot electrons) is analyzed with a new kinetic model, focusing on the influence of the electron dynamics. Simple, general laws are found, relating the key expansion features to the initial conditions of the plasma. A transition is identified in the shape of the ion energy spectrum, which is monotonic only for high electron temperatures, otherwise exhibiting a local peak far from the cutoff energy.

1. INTRODUCTION

Recent experiments on the interaction of ultraintense laser pulses with clusters [1] have shown the possibility of accelerating ions to energies of interest for many applications, such as nuclear fusion and x-ray generation. For applications requiring an accurate control over the expansion dynamics (e.g., double-pump experiments for inducing intracluster reactions [2], or interactions of x-ray pulses with biological samples for imaging purposes [3]), a detailed knowledge of the kinetics of the expansion is necessary. To this end, the collisionless expansion of spherical plasmas, composed of cold ions and hot electrons, is analyzed using a new Lagrangian model [4], which allows a kinetic description of the radial ion motion and of the three-dimensional electron motion. The case of initially-Maxwellian electrons is investigated in detail for a wide range of initial conditions, and simple relationships are deduced for the key expansion features. The study also reveals peculiarities of the ion energy spectrum (formation of a local maximum and transition from nonmonotonic to monotonic behaviour), not taken into account by simple Coulomb explosion (CE) models and potentially important for the interpretation of experiments where single-cluster effects are relevant.

2. ERGODIC MODEL FOR THE EXPANSION

The expansion process is divided in two stages: a rapid expansion of the electrons (charging transient), which leads to an equilibrium configuration before the ions move appreciably, and a subsequent, slower expansion of the plasma bulk. The electron distribution is described as a sequence of ergodic equilibrium configurations, so that the only independent variable related to the electrons is their total energy $\varepsilon = m_e \mathbf{v}^2 / 2 - e\Phi$. The ions move radially (starting from r_0) and the electrons change energy (starting from ε_0). The model determines the ion trajectories $r_i(r_0, t)$, the electron energies $\varepsilon(\varepsilon_0, t)$, the ion density $n_i(r, t)$, the electron density $n_e(r, t)$, and the potential $\Phi(r, t)$, according to the set of equations

$$\left\{ \begin{array}{l} m_i \frac{\partial^2 r_i}{\partial t^2} = -Ze \frac{\partial \Phi}{\partial r}(r_i) \\ \frac{1}{r^2} \frac{\partial}{\partial r} \left(r^2 \frac{\partial \Phi}{\partial r} \right) = 4\pi e (n_e - Zn_i) \\ n_i(r_i) = n_{i,0}(r_0) \frac{r_0^2}{r_i^2} \frac{\partial r_i}{\partial r_0} \\ n_e = \frac{1}{4\pi r^2} \int \rho_0(\varepsilon_0) \wp(r; \varepsilon) d\varepsilon_0 \\ \frac{d\varepsilon}{dt} = -e \int \frac{\partial \Phi}{\partial t} \wp(r; \varepsilon) dr \end{array} \right. \quad \begin{array}{l} (1a) \\ (1b) \\ (1c) \\ (1d) \\ (1e) \end{array}$$

where m_i is the ion mass and Z the ion charge state. The expansion dynamics is determined once the initial ion density $n_{i,0}$ and the electron energy distribution ρ_0 are given. In Eqs. (1d) and (1e), $\wp(r; \varepsilon) = r^2 \sqrt{\varepsilon + e\Phi} / \int r'^2 \sqrt{\varepsilon + e\Phi(r')} dr'$ is the probability density of finding an electron with energy ε at the radius r . As can be noticed by writing Eqs. (1) in dimensionless form, the dynamics of the expansion depends on the single parameter $\hat{T}_0 = Zk_B T_0 / \varepsilon_{CE}$, being $\varepsilon_{CE} = Ze^2 N_0 / R_0$ the maximum ion energy attainable from the CE of a uniformly-charged sphere of ions, with radius R_0 and total charge eN_0 . The initial equilibrium is determined by introducing a rigid potential barrier and gradually moving it outward, taking special care to avoid energy exchanges between the electrons and the expanding barrier. The validity of this procedure has been tested by using reference results from particle-in-cell (PIC) simulations performed with the OSIRIS 2.0 framework [5].

3. INITIAL EQUILIBRIUM

In Fig. 1 the equilibrium electron density and electric field are shown and compared with results from PIC simulations, for $\hat{T}_0 = 7.2 \times 10^{-3}$ and $\hat{T}_0 = 7.2 \times 10^{-2}$.

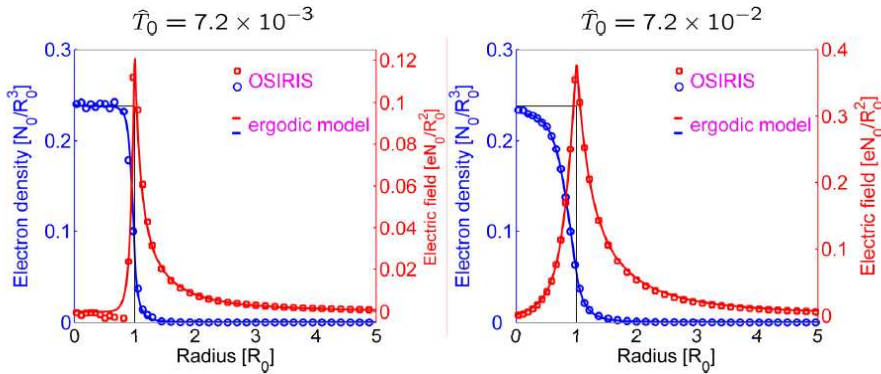


FIG. 1: Electron density (blue) and electric field (red), after the initial charging transient.

Figure 2 shows the equilibrium charge buildup within the ion core and the total kinetic energy of trapped electrons, as functions of \hat{T}_0 . Both quantities admit accurate, simple fit laws, valid for any value of \hat{T}_0 (which reduce to power-law behaviours at low \hat{T}_0).

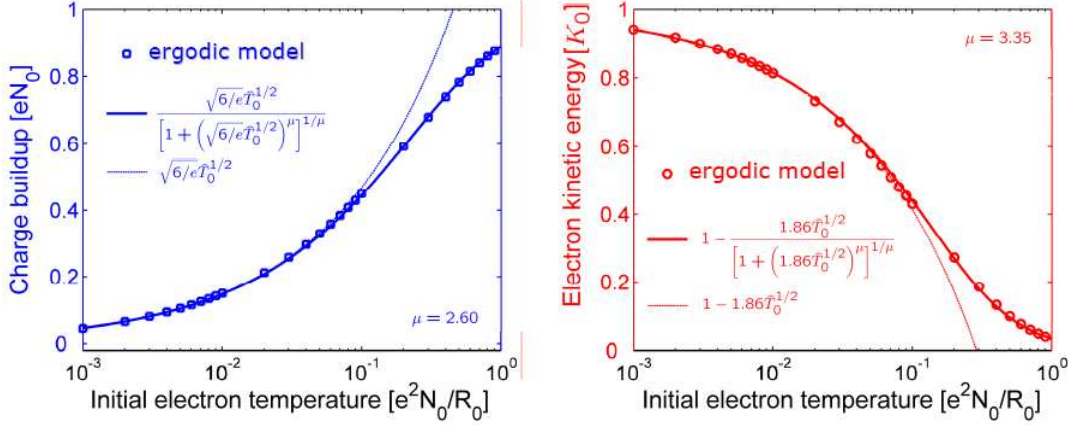


FIG. 2: Charge buildup within the ion core (blue) and total kinetic energy of trapped electrons (red) as functions of \hat{T}_0 , after the initial charging transient. Circles refer to the present theory, while solid lines refer to the displayed fit laws. Thin lines show the power-law behaviours in the low-temperature regime. K_0 is the initial total kinetic energy of the electrons.

4. BULK EXPANSION

When the ions start moving, the electrons rapidly cool down and move towards the centre of the distribution, trying to restore charge neutrality, as illustrated in Fig. 3.

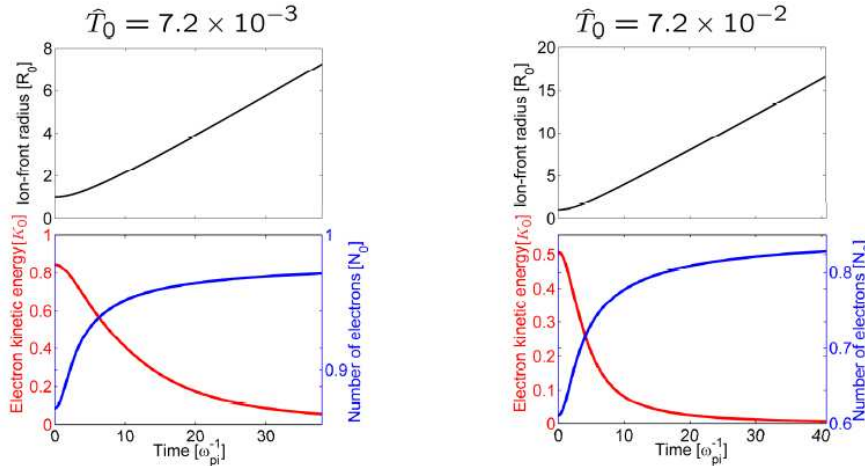


FIG. 3: Evolution of the number of electrons (blue) within the instantaneous radius of the ion front (black), and of the total kinetic energy of trapped electrons (red).

This behaviour strongly affects the ion energy spectrum. In fact, the asymptotic energy ε_∞ of an ion starting at r_0 is given by

$$\frac{\varepsilon_\infty(r_0)}{Ze} = \frac{q(r_0, 0)}{r_0} + \int_0^\infty \frac{1}{r_i(r_0, t)} \frac{\partial q(r_i(r_0, t), t)}{\partial t} dt, \quad (2)$$

where q is the net charge buildup within a sphere of radius r at time t . The integral term (vanishing for a CE) accounts for the energy loss due to the decrease of positive charge buildup experienced by each ion along its trajectory. The shape of the asymptotic energy spectrum and its cutoff energy depend strongly on the initial conditions, as shown in Fig. 4: for $\hat{T}_0 < 0.5$, the spectrum exhibits a maximum far from the energy cutoff. Such distribution is qualitatively and quantitatively different from the asymptotic spectrum of a pure CE. $\hat{T}_0 = 0.5$ can hence be taken as a lower bound for the validity of the CE model.

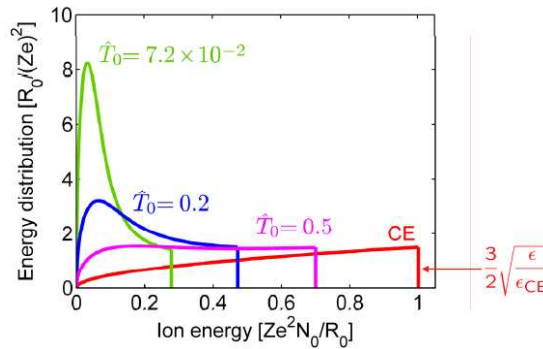


FIG. 4: Asymptotic ion energy spectra for different \hat{T}_0 . The red curve refers to the pure CE case.

The cutoff ion energy ϵ_{\max} as a function of \hat{T}_0 is shown in Fig. 5, along with the energy corresponding to the peak in the spectrum. Simple fit laws are found also for these quantities.

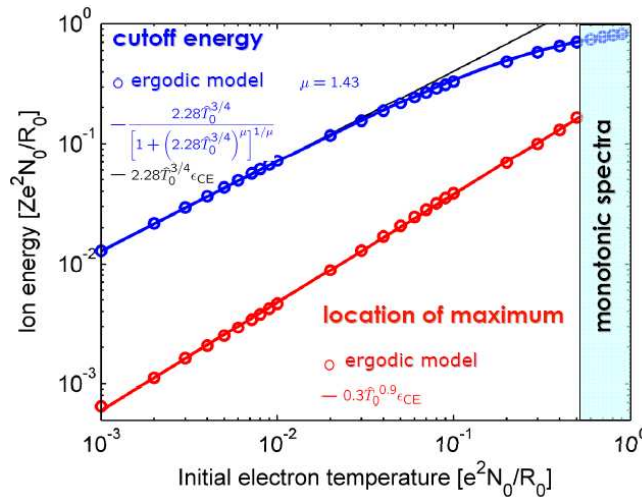


FIG. 5: Cutoff ion energy (blue) and location of the maximum in the ion energy spectrum (red) as functions of \hat{T}_0 : circles refer to the present theory, while solid lines refer to the displayed fit laws.

REFERENCES

[1] T. Ditmire *et al.*, Nature **386**, 54 (1997); T. Ditmire *et al.*, Nature **398**, 489 (1999).
 [2] F. Peano *et al.*, Phys. Rev. Lett. **94**, 033401 (2005); Phys. Rev. A **73**, 053202 (2006).
 [3] R. Neutze *et al.*, Nature **406**, 752 (2000); H. Wabnitz *et al.*, Nature **420**, 482 (2002).
 [4] F. Peano *et al.*, Phys. Rev. Lett. **96**, 175002 (2006).
 [5] R.A. Fonseca *et al.*, Lect. Notes Comp. Sci. **2329**, (Springer-Verlag, Heidelberg, 2002) p. 342.